Acta Crystallographica Section A
Foundations of Crystallography
ISSN 0108-7673

Received 14 December 2009
Accepted 24 March 2010

Two-wave approximation in surface effects in asymmetric Laue crystals

M. Guida[a] and C. Palmisano[b,a]*

[a]Università di Torino, Dipartimento di Fisica Generale 'A. Avogadro', via P. Giuria 1, 10125 Torino, Italy, and [b]Museo Storico della Fisica e Centro Studi e Ricerche 'Enrico Fermi', Piazza del Viminale 1, 00184 Roma, Italy. Correspondence e-mail: palmisan@to.infn.it

This paper is a study of surface effects, *e.g.* roughness or asymmetrical cut, in the Laue diffraction of X-rays by crystals, based on the Takagi–Taupin equations. By means of Riemann–Green integrals, first a formal solution has been obtained when the entrance and the exit surfaces are arbitrary. Then a coordinate transformation mapping a propagation domain with arbitrary boundaries into a rectangular domain with straight boundaries is given. Potential measurement errors in γ-ray wavelength and silicon lattice-parameter measurements by double-crystal diffractometry and X-ray interferometry, respectively, are outlined and anticipated by studying, in the two-wave approximation, the reflection peak shift and extra phase originating from an asymmetrically cut crystal. A relationship between analyser displacement, interferometer-signal phase and relative uncertainty in lattice-parameter measurement is also given.

1. Introduction

To determine the Avogadro constant to an accuracy allowing a redefinition of the kilogram to be based on an atomic standard and fundamental constants (Becker, 2003; Flowers, 2004; Mills *et al.*, 2005; Robinson, 2006; Becker, De Bièvre *et al.*, 2007; Becker, Jentschel *et al.*, 2007), the relative uncertainties of the ^{28}Si lattice parameter and of the binding energy of a neutron in the ^{36}Cl nucleus must be reduced to 3×10^{-9} and 5×10^{-8}, respectively. The measurements of these quantities depend upon the diffraction of X-rays and γ-rays in crystals, through experiments based on X-ray interferometry and γ-ray spectroscopy (Materna *et al.*, 2006), respectively.

In an X-ray interferometer, the fringe phase in addition to the wanted lattice parameter records also the roughness of the crystal surface (Massa *et al.*, 2009). Similarly, in a double-crystal diffractometer (Becker, Jentschel *et al.*, 2007), the angular separation between the dispersive and the non-dispersive diffraction peaks, in addition to the wanted γ-ray wavelength, records also the asymmetry of the crystal surfaces. Although these asymmetries and surface effects are weaker by orders of magnitude than the known dynamical diffraction ones, at the required sensitivity level they influence measurement results. Therefore, to separate ghosts from reality, it is necessary to investigate the contribution of the surface geometry to the diffraction of X-rays and γ-rays by crystals.

In this paper, we model the X-ray diffraction in crystals without making any restricting assumptions on the shape of the crystal surfaces. This work is aimed at providing a tool for the analysis of anomalies (Massa *et al.*, 2005, 2009) which might originate in the crystal surface, but which are not yet clearly explained in that way. Our goal is to set the theoretical framework necessary to investigate numerically, in subsequent papers, the systematic errors owing to imperfect surface geometry in the measurement of γ-ray wavelengths and the lattice parameter.

In §2, a two-dimensional crystal model, the relevant Takagi–Taupin equations and useful domain transformations are considered. Next, in §3, the equivalence between two different approaches to take account of the small crystal rotation is demonstrated; furthermore, the formalism used by Apolloni *et al.* (2008) to study X-ray propagation in cylindrical crystals is extended to arbitrary surfaces by a coordinate transformation, which maps a propagation domain having arbitrary boundaries into a rectangular one with straight boundaries. In §4, a formula for the link between the 'deviation of the reflection-domain centre from the Bragg angle' and 'the asymmetry angle' is re-obtained by using analytical methods. Finally, to outline in the simplest way the study of double-crystal diffractometers and X-ray interferometers and to anticipate the potential measurement errors, §5 discusses in detail the reflection peak shift and extra phase originated by an asymmetrically cut crystal.

2. Takagi–Taupin equations

In order to study the Laue diffraction of X-rays in crystals, we use the Takagi–Taupin equations (Takagi, 1962, 1969; Taupin, 1964; Authier, 2005; Mana & Montanari, 2004) in the two-wave approximation of the dynamical theory of X-ray diffraction. We shall use a two-dimensional model having a reference frame whose origin is on the entrance crystal surface. Even though only perfect crystals will be considered,

we write the Takagi–Taupin equations in a general form, with a lattice distortion term included, since this will help the study of crystal rotations as a kind of lattice distortion. Lattice distortion is described by the displacement field $\mathbf{u}(x, z)$, which gives the distance between a point of the distorted lattice and the same point of a reference perfect lattice, this lattice being chosen by setting the x axis parallel to the reciprocal vector $\mathbf{h}_0$ and the z axis parallel to the Bragg planes.

Let us introduce the Ewald expansion of the dielectric displacement vector $\mathbf{D} = D\hat{\mathbf{y}}$ in σ polarization,

$$D = D_\mathrm{o} \exp(i\,\mathbf{K}_\mathrm{o} \cdot \mathbf{r}) + D_\mathrm{h} \exp\big[i(\mathbf{K}_\mathrm{h} \cdot \mathbf{r} - \mathbf{h}_0 \cdot \mathbf{u})\big]. \quad (1)$$

Next, if we introduce two new amplitudes d_o and d_h (Apolloni *et al.*, 2008) defined as

$$d_{\mathrm{o,h}} = \exp\left(-i\frac{K\chi_\mathrm{o}}{2}\frac{\hat{\mathbf{s}}_\mathrm{o} + \hat{\mathbf{s}}_\mathrm{h}}{1 + \hat{\mathbf{s}}_\mathrm{o} \cdot \hat{\mathbf{s}}_\mathrm{h}} \cdot \mathbf{r}\right) D_{\mathrm{o,h}} \quad (2)$$

(note that $K\chi_\mathrm{o}/2$ is the variation of the wavenumber induced by the index of refraction, and the complete term $K(\chi_\mathrm{o}/2)(\hat{\mathbf{s}}_\mathrm{o} + \hat{\mathbf{s}}_\mathrm{h})/(1 + \hat{\mathbf{s}}_\mathrm{o} \cdot \hat{\mathbf{s}}_\mathrm{h})$ is the vector connecting the Lorentz and Laue points), the Takagi–Taupin equations can be rewritten as

$$-i\,\hat{\mathbf{s}}_\mathrm{o} \cdot \nabla d_\mathrm{o} = \frac{K\chi_\mathrm{h}}{2} d_\mathrm{h}, \quad (3)$$

$$-i\,\hat{\mathbf{s}}_\mathrm{h} \cdot \nabla d_\mathrm{h} = \frac{K\chi_\mathrm{h}}{2} d_\mathrm{o} + \big[\hat{\mathbf{s}}_\mathrm{h} \cdot \nabla(\mathbf{h}_0 \cdot \mathbf{u})\big] d_\mathrm{h}, \quad (4)$$

where $\hat{\mathbf{s}}_\mathrm{o} = \hat{\mathbf{K}}_\mathrm{o} = -\sin\theta_\mathrm{B}\hat{\mathbf{x}} + \cos\theta_\mathrm{B}\hat{\mathbf{z}}$ and $\hat{\mathbf{s}}_\mathrm{h} = \hat{\mathbf{K}}_\mathrm{h} = \sin\theta_\mathrm{B}\hat{\mathbf{x}} + \cos\theta_\mathrm{B}\hat{\mathbf{z}}$ are unit propagation vectors, θ_B being the Bragg angle (with a sign), $\mathbf{h}_0 = 2K\sin\theta_\mathrm{B}\hat{\mathbf{x}}$, $\mathbf{K}_\mathrm{h} = \mathbf{K}_\mathrm{o} + \mathbf{h}_0$, $K = \|\mathbf{K}_\mathrm{o}\| = \|\mathbf{K}_\mathrm{h}\| = 2\pi\nu/c$ is the modulus of the wavenumber vector $\mathbf{K}_\mathrm{e}$ of the incoming radiation (with frequency ν), and the complex parameters χ_o, χ_h and $\chi_{-\mathrm{h}}$ are the Fourier components of electric susceptibility. As we are interested in silicon crystals, we shall study only the case $\chi_{-\mathrm{h}} = \chi_\mathrm{h}$.

2.1. Crystal surfaces

We shall consider a monochromatic source, having finite width (1 mm), and illuminating at the exact Bragg condition an infinite crystal slab, the surfaces of which are smooth curves in the reflection plane (Fig. 1). They will be denoted $\mathbf{\Gamma}(\tau)$ on the entrance surface and $\mathbf{\Sigma}(\sigma)$ on the exit surface, and given in a parametric form as $[\Gamma_x = \tau,\ \Gamma_z = f_1(\tau)]$, and $[\Sigma_x = \sigma,\ \Sigma_z = T + f_2(\sigma)]$, where f_1 and f_2 are arbitrary differentiable functions and T is a parameter which reduces to the thickness when $f_1 = f_2 = 0$. By requiring $f_1(\tau) < T + f_2(\tau)$, we prevent any intersection between the curves $\mathbf{\Gamma}$ and $\mathbf{\Sigma}$. The parameters of the curves have been chosen in such a way to have a realistic representation of the surfaces; see, for example, Fig. 4 of Massa *et al.* (2009). Two-dimensional boundaries and coupling to other diffracted waves should in principle be taken into account, but they cannot be treated within this formalism and will be studied in subsequent papers. However, our mathematical treatment can be easily extended to piecewise smooth curves.

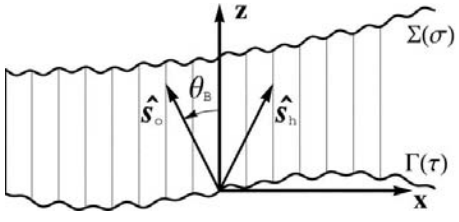

Figure 1
Example of a crystal slab with rough entrance surface $\Gamma(\tau)$ and rough exit surface $\Sigma(\sigma)$. The unit propagation vectors $\hat{\mathbf{s}}_\mathrm{o}$ and $\hat{\mathbf{s}}_\mathrm{h}$ and the oriented Bragg angle θ_B are also shown. The vertical lines represent the Bragg planes.

2.2. Initial conditions

Strictly speaking, we should study a three-dimensional model and impose the continuity of the tangential component (parallel to the external surface) of the electric field and of the orthogonal component of the dielectric displacement field. However, since we are considering a two-dimensional model and only σ polarization, we shall assume $(1 + \chi) \simeq 1$ and impose the continuity of the dielectric displacement field. Then, under the hypothesis that at each point of the entrance surface the field $D(\mathbf{r})$ in equation (1) is equal to the incoming wave

$$D_\mathrm{o} \exp(i\mathbf{K}_\mathrm{o} \cdot \mathbf{r})|_\Gamma = A(x, z) \exp(i\mathbf{K}_\mathrm{e} \cdot \mathbf{r})|_\Gamma, \quad (5)$$

the initial conditions are

$$d_\mathrm{o}(x, z)|_\Gamma = \exp\left(-i\frac{K\chi_\mathrm{o}}{2}\frac{\hat{\mathbf{s}}_\mathrm{o} + \hat{\mathbf{s}}_\mathrm{h}}{1 + \hat{\mathbf{s}}_\mathrm{o} \cdot \hat{\mathbf{s}}_\mathrm{h}} \cdot \mathbf{r}\right) \mathbf{\Phi}(x, z)|_\Gamma \quad (6)$$

$$d_\mathrm{h}(x, z)|_\Gamma = 0, \quad (7)$$

where

$$\Phi(x, z)|_\Gamma = A(x, z) \exp\big[i(\mathbf{K}_\mathrm{e} - \mathbf{K}_\mathrm{o}) \cdot \mathbf{r}\big]|_\Gamma. \quad (8)$$

We recall that we have chosen $\|\mathbf{K}_\mathrm{e}\| = \|\mathbf{K}_\mathrm{o}\| = 2\pi\nu/c$, without assuming any hypothesis about the continuity of the tangential components of the wavevectors; furthermore, the vector $\mathbf{K}_\mathrm{o}$ has been defined as satisfying the Bragg law independently of the direction of incidence of the incoming field. However, in some cases we shall exploit the choice $\mathbf{K}_\mathrm{o} = \mathbf{K}_\mathrm{e}$. A discussion about other possible choices, such as $\|\mathbf{K}_\mathrm{o}\| = n\|\mathbf{K}_\mathrm{e}\|$ with n the index of refraction, and the relevant form of the equations and the initial conditions can be found in Gronkowski (1991).

2.3. The Riemann–Green method

A solution of (3, 4), with $\mathbf{u} = 0$ and initial conditions (6, 7), can be found by quadrature *via* the Riemann–Green method (Sommerfeld, 1964; Authier & Simon, 1968; Takagi, 1969; Thorkildsen & Larsen, 1998); hence,

$$d_{\mathrm{o,h}}(x, z) = \int_\Gamma G_{\mathrm{o,h}}(x - \Gamma_x, z - \Gamma_z)\, d_\mathrm{o}(\Gamma_x, \Gamma_z)\, \frac{\hat{\mathbf{s}}_\mathrm{o} \cdot \hat{\mathbf{n}}_\Gamma}{\cos\theta_\mathrm{B}}\, \mathrm{d}\Gamma, \quad (9)$$

where the unit vector $\hat{\mathbf{n}}_\Gamma = [-(\mathrm{d}\Gamma_z/\mathrm{d}\tau)\,\hat{\mathbf{x}} + \hat{\mathbf{z}}]/[1 + (\mathrm{d}\Gamma_z/\mathrm{d}\tau)^2]^{1/2}$ is the inward normal to $\mathbf{\Gamma}$ and $\mathrm{d}\Gamma$ is a shorthand form for

$\|\mathrm{d}\boldsymbol{\Gamma}/\mathrm{d}\tau\|\,\mathrm{d}\tau$. By use of the same notation as Palmisano & Zosi (2005), the kernels G_o and G_h in (9) are

$$\begin{aligned} G_\mathrm{o}(x,z) = {} & \delta(x + z\tan\theta_\mathrm{B}) - \frac{K}{4|\sin\theta_\mathrm{B}|}(\chi_\mathrm{h}\chi_{-\mathrm{h}})^{1/2} \\ & \times \mathrm{H}(z|\tan\theta_\mathrm{B}| + x)\,\mathrm{H}(z|\tan\theta_\mathrm{B}| - x) \\ & \times \left(\frac{z\tan\theta_\mathrm{B} - x}{z\tan\theta_\mathrm{B} + x}\right)^{1/2} \\ & \times J_1\left[\frac{K}{2|\sin\theta_\mathrm{B}|}(\chi_\mathrm{h}\chi_{-\mathrm{h}})^{1/2}\left(z^2\tan^2\theta_\mathrm{B} - x^2\right)^{1/2}\right] \end{aligned} \tag{10}$$

and

$$\begin{aligned} G_\mathrm{h}(x,z) = {} & \frac{i}{4}\frac{K\chi_\mathrm{h}}{|\sin\theta_\mathrm{B}|}\,\mathrm{H}(z|\tan\theta_\mathrm{B}| + x)\,\mathrm{H}(z|\tan\theta_\mathrm{B}| - x) \\ & \times J_0\left[\frac{K}{2|\sin\theta_\mathrm{B}|}(\chi_\mathrm{h}\chi_{-\mathrm{h}})^{1/2}\left(z^2\tan^2\theta_\mathrm{B} - x^2\right)^{1/2}\right], \end{aligned} \tag{11}$$

where $\mathrm{H}(z)$ is the Heaviside function and $J_0(z)$ and $J_1(z)$ are the Bessel functions of the first kind and order 0 and 1, respectively.

2.4. Domain transformation

An alternative to the computation of formula (9) is to solve the equations (3) and (4) numerically. To avoid the problem of assigning the initial conditions on an arbitrary surface, when $f_1(x) \le z \le T + f_2(x)$, we introduce the propagation coordinate

$$\eta = T\,\frac{z - f_1(x)}{T + f_2(x) - f_1(x)}. \tag{12}$$

In this way the crystal surfaces are given by $\Gamma_x = \tau$ and $\Gamma_\eta = 0$, and $\Sigma_x = \sigma$ and $\Sigma_\eta = T$, that is, the transformation (12) maps a domain having irregular boundaries into a rectangular one. The inverse transformation can easily be calculated; it is

$$z = f_1(x) + (\eta/T)\big[T + f_2(x) - f_1(x)\big]. \tag{13}$$

By applying the chain rule to equations (3) and (4), *i.e.* $\partial/\partial z = (\partial\eta/\partial z)\partial/\partial\eta$ and similar expressions, and exploiting the elements of the Jacobian matrix J,

$$\begin{aligned} J(x,\eta) &= \begin{pmatrix} \partial x/\partial x & \partial x/\partial z \\ \partial\eta/\partial x & \partial\eta/\partial z \end{pmatrix} \\ &= \begin{pmatrix} 1 & 0 \\ \dfrac{(\eta - T)f_1'(x) - \eta f_2'(x)}{T + f_2(x) - f_1(x)} & \dfrac{T}{T + f_2(x) - f_1(x)} \end{pmatrix}, \end{aligned} \tag{14}$$

we have

$$\begin{aligned} & -\sin\theta_\mathrm{B}\frac{\partial\tilde{d}_\mathrm{o}}{\partial x} + \frac{T\cos\theta_\mathrm{B} - [(\eta - T)f_1'(x) - \eta f_2'(x)]\sin\theta_\mathrm{B}}{T + f_2(x) - f_1(x)}\frac{\partial\tilde{d}_\mathrm{o}}{\partial\eta} \\ & \quad = (i/2)\,K\chi_{-\mathrm{h}}\tilde{d}_\mathrm{h}, \end{aligned} \tag{15}$$

$$\begin{aligned} & \sin\theta_\mathrm{B}\frac{\partial\tilde{d}_\mathrm{h}}{\partial x} + \frac{T\cos\theta_\mathrm{B} + \big[(\eta - T)f_1'(x) - \eta f_2'(x)\big]\sin\theta_\mathrm{B}}{T + f_2(x) - f_1(x)}\frac{\partial\tilde{d}_\mathrm{h}}{\partial\eta} \\ & \quad = (i/2)\,K\chi_\mathrm{h}\tilde{d}_\mathrm{o} + i\big[\hat{\mathbf{s}}_\mathrm{h}\cdot\nabla_{(x,z)}(\mathbf{h}_0\cdot\mathbf{u})\big]\tilde{d}_\mathrm{h}, \end{aligned} \tag{16}$$

where $\tilde{d}_\mathrm{o} = d_\mathrm{o}[x, z(x,\eta)]$, $\tilde{d}_\mathrm{h} = d_\mathrm{h}[x, z(x,\eta)]$. In this case, the initial conditions (6) and (7) become

$$\tilde{d}_\mathrm{o}(x,0) = \exp\left[-i\frac{K\chi_\mathrm{o}}{2\cos\theta_\mathrm{B}}\,f_1(x)\right]\Phi[x, f_1(x)], \tag{17}$$

$$\tilde{d}_\mathrm{h}(x,0) = 0, \tag{18}$$

where we chose $\mathbf{K}_\mathrm{e} = \mathbf{K}_\mathrm{o}$. The subscript in $\nabla_{(x,z)}$ indicates that $\mathbf{h}_0\cdot\mathbf{u}$ must be differentiated with respect to the x and z variables. The initial propagation coordinate can be restored in the solutions of (15) and (16) by inverse transformation (13). Hence,

$$\begin{aligned} D_{\mathrm{o,h}}|_\Sigma &= D_{\mathrm{o,h}}\big[x, T + f_2(x)\big] \\ &= \exp\left\{i\frac{K\chi_\mathrm{o}}{2\cos\theta_\mathrm{B}}\Big[T + f_2(x)\Big]\right\}\tilde{d}_{\mathrm{o,h}}(x, \eta = T), \end{aligned} \tag{19}$$

where the definition (2) has been used.

3. Small crystal rotations

In this section we shall study two equivalent methods to treat small deviations of the incoming beam from the exact Bragg condition, either by considering a small rotation of the whole crystal or by inserting a distortion term into equation (4). In the first approach we shall have a change of the initial conditions and an extra phase term in the Ewald expansion (1); this latter term is generated by a change of reference frame. In the second, in order to demonstrate the just mentioned equivalence, we shall eliminate the distortion term by a change of dependent variables and obtain the same initial conditions as in the first approach. Finally, we shall demonstrate that the two Ewald expansions coincide.

In the last subsection we shall see how to eliminate the distortion term in the domain transformation approach.

3.1. Equivalence between rotation and distortion

A crystal rotation by an angle α around an axis orthogonal to the reflection plane is equivalent to a rotation of the incoming X-ray beam by an angle $-\alpha$. Consequently, in the crystal reference frame the Ewald expansion (1) and the Takagi–Taupin equations (3) and (4), where $[\hat{\mathbf{s}}_\mathrm{h}\cdot\nabla(\mathbf{h}_0\cdot\mathbf{u})]$ vanishes because we are considering a perfect crystal, are left unchanged, but the initial conditions have to be modified accordingly. When we start from the incoming wave (5), equation (8) becomes

$$\Phi(x,z)|_\Gamma = A(x,z)|_{\Gamma'}\exp\big[i(\mathbf{K}_\mathrm{e}' - \mathbf{K}_\mathrm{o})\cdot\mathbf{r}\big]|_\Gamma, \tag{20}$$

where $\boldsymbol{\Gamma}' = \mathbf{R}(\alpha)\boldsymbol{\Gamma}$ is the entrance surface rotated by an angle α, $\mathbf{R}(\alpha)$ being the relevant rotation matrix,

$$\mathbf{R}(\alpha) = \begin{pmatrix} \cos\alpha & \sin\alpha \\ -\sin\alpha & \cos\alpha \end{pmatrix}, \tag{21}$$

and $\mathbf{K}'_{\rm e} = \mathbf{R}(-\alpha)\mathbf{K}_{\rm e}$ is the incoming wavevector rotated by an angle $-\alpha$. Note that, according to definition (19), clockwise rotations correspond to positive angles. Let us choose $\mathbf{K}_{\rm e} = \mathbf{K}_{\rm o}$. Since second-order terms such as α^2 can be neglected, so can $\mathbf{K}'_{\rm e} - \mathbf{K}_{\rm o} \simeq -\alpha(K_{{\rm o},z}\hat{\mathbf{x}} - K_{{\rm o},x}\hat{\mathbf{z}})$, and since, in addition, the transverse width of the incoming X-ray beam and the crystal-boundary deviation from the x axis are small enough to allow the approximation $A(x, z)|_{\Gamma'} \simeq A(x, z)|_{\Gamma}$ to be made, then equation (6) becomes

$$d_{\rm o}(x, z)|_{\Gamma} \simeq \exp\left(-i\frac{K\chi_{\rm o}}{2}\frac{\hat{\mathbf{s}}_{\rm o} + \hat{\mathbf{s}}_{\rm h}}{1 + \hat{\mathbf{s}}_{\rm o}\cdot\hat{\mathbf{s}}_{\rm h}}\cdot\mathbf{r}\right)|_{\Gamma} A(\Gamma_x, \Gamma_z) \times \exp\left[-i\alpha\left(K_{{\rm o},z}\Gamma_x - K_{{\rm o},x}\Gamma_z\right)\right]. \quad (22)$$

Eventually, by using equation (2) for the inverse transformation $d_{\rm o,h} \rightarrow D_{\rm o,h}$, and by use of the substitutions $x = (x^{\rm lab} - \alpha z^{\rm lab})$ and $z = (z^{\rm lab} + \alpha x^{\rm lab})$ in the exponential terms of equation (1), we obtain

$$D = D_{\rm o}\exp\left[i\,\mathbf{K}_{\rm o}\cdot\mathbf{r} + iK\alpha(x\cos\theta_{\rm B} + z\sin\theta_{\rm B})\right] + D_{\rm h}\exp\left[i\,\mathbf{K}_{\rm h}\cdot\mathbf{r} + iK\alpha(x\cos\theta_{\rm B} - z\sin\theta_{\rm B})\right], \quad (23)$$

which is the Ewald expansion in term of the coordinates x and z, the superscript 'lab' having been omitted, of the laboratory reference frame.

Now we can show how this approach is equivalent to considering small rotations of the whole crystal as a very special kind of distortion, even in the case of surfaces with arbitrary shape. Indeed, let us assume firstly that $\mathbf{h}_0$ is independent of rotations; secondly, that, as the origin of the reference frame is on the entrance surface, the rotation displacement is

$$\mathbf{u}^{\rm rot}(x, z) = (\hat{\mathbf{x}}, \hat{\mathbf{z}})[\mathbf{R}(\alpha) - \mathbf{1}]\begin{pmatrix} x \\ z \end{pmatrix}, \quad (24)$$

where $\mathbf{1}$ is the identity matrix of size 2, and can be approximated by

$$\mathbf{u}^{\rm rot}(x, z) \simeq \alpha z\hat{\mathbf{x}} - \alpha x\hat{\mathbf{z}}; \quad (25)$$

thirdly, that the crystal surfaces are left unchanged by rotations. From equation (25) we find the explicit expression

$$\hat{\mathbf{s}}_{\rm h}\cdot\nabla(\mathbf{h}_0\cdot\mathbf{u}^{\rm rot}) = 2K\alpha\sin\theta_{\rm B}\cos\theta_{\rm B}, \quad (26)$$

for the last term in equation (4) when $\mathbf{u} = \mathbf{u}^{\rm rot}$. By a change of the dependent variable, this distortion term $\hat{\mathbf{s}}_{\rm h}\cdot\nabla(\mathbf{h}_0\cdot\mathbf{u}^{\rm rot})$ can be eliminated in equation (4), and the effect of rotation about the vertical axis can be included in new initial conditions. Let us introduce the two unknowns $\hat{d}_{\rm o}$ and $\hat{d}_{\rm h}$ defined as

$$\hat{d}_{\rm o,h} = \exp\left[-i\,2K\sin\theta_{\rm B}\,f(x, z)\right]d_{\rm o,h}, \quad (27)$$

where

$$f(x, z) = \frac{\alpha}{2}\cos\theta_{\rm B}\left(\frac{x}{\sin\theta_{\rm B}} + \frac{z}{\cos\theta_{\rm B}}\right), \quad (28)$$

and substitute into equations (3) and (4); the Takagi–Taupin equations then reduce to the unperturbed form, which can be solved by the Riemann–Green method,

$$-i\,\hat{\mathbf{s}}_{\rm o}\cdot\nabla\hat{d}_{\rm o} = \frac{K\chi_{-\rm h}}{2}\,\hat{d}_{\rm h}, \quad (29)$$

$$-i\,\hat{\mathbf{s}}_{\rm h}\cdot\nabla\hat{d}_{\rm h} = \frac{K\chi_{h}}{2}\,\hat{d}_{\rm o}, \quad (30)$$

with the initial conditions

$$\hat{d}_{\rm o}(x, z)|_{\Gamma} = \exp\left[-i\alpha\left(K_{\rm o}, z\Gamma_x - K_{\rm o}, x\Gamma_z\right)\right] \times \exp\left(-i\frac{K\chi_{\rm o}}{2}\frac{\hat{\mathbf{s}}_{\rm o} + \hat{\mathbf{s}}_{\rm h}}{1 + \hat{\mathbf{s}}_{\rm o}}\cdot\hat{\mathbf{s}}_{\rm h}\cdot\mathbf{r}\right)|_{\Gamma} A\left(\Gamma_x, \Gamma_z\right), \quad (31)$$

$$\hat{d}_{\rm h}(x, z)|_{\Gamma} = 0. \quad (32)$$

To obtain equation (31) we have exploited the choice $\mathbf{K}_{\rm e} = \mathbf{K}_{\rm o}$, the equality $(K_{{\rm o},x}, K_{{\rm o},z}) = (-K\sin\theta_{\rm B}, K\cos\theta_{\rm B})$, and equations (6), (8), (27) and (28). We remark that the initial conditions (22) and (31) are identical and, after applying the inverse transformation $\hat{d}_{\rm o,h} \rightarrow d_{\rm o,h} \rightarrow D_{\rm o,h}$ and substitution of $D_{\rm o,h}$ in equation (1), the Ewald expansion coincides with equation (23). Hence the two approaches, crystal rotation and lattice-plane distortion, are equivalent as long as the approximations about α, Γ and Σ remain valid.

3.2. Different methods: integral and differential

By using the Riemann–Green method (§2.3) to solve system (29) and (30) with the initial conditions (31) and (32) and by using equations (27) and (2) for the inverse transformation $\hat{d}_{\rm o,h} \rightarrow d_{\rm o,h} \rightarrow D_{\rm o,h}$, we find the explicit solution to system (29, 30), calculated on the exit surface Σ, for the two fields in the Ewald expansion (1),

$$\begin{aligned} D_{\rm o,h}(x, z; \alpha)|_{\Sigma} = {} & \exp\left[i\frac{K\chi_{\rm o}}{2}\frac{\hat{\mathbf{s}}_{\rm o} + \hat{\mathbf{s}}_{\rm h}}{1 + \hat{\mathbf{s}}_{\rm o}\cdot\hat{\mathbf{s}}_{\rm h}}\cdot(\Sigma_x\hat{\mathbf{x}} + \Sigma_z\hat{\mathbf{z}})\right] \\ & \times \exp\left[i\alpha\left(K_{{\rm o},z}\Sigma_x - K_{{\rm o},x}\Sigma_z\right)\right] \\ & \times \int_{\Gamma} G_{\rm o,h}(x - \Gamma_x, z - \Gamma_z) \\ & \times \exp\left[-i\alpha\left(K_{{\rm o},z}\Gamma_x - K_{{\rm o},x}\Gamma_z\right)\right] \\ & \times \exp\left[-i\frac{K\chi_{\rm o}}{2}\frac{\hat{\mathbf{s}}_{\rm o} + \hat{\mathbf{s}}_{\rm h}}{1 + \hat{\mathbf{s}}_{\rm o}\cdot\hat{\mathbf{s}}_{\rm h}}\cdot\left(\Gamma_x\hat{\mathbf{x}} + \Gamma_z\hat{\mathbf{z}}\right)\right] \\ & \times A\left(\Gamma_x, \Gamma_z\right)\frac{\hat{\mathbf{s}}_{\rm o}\cdot\hat{\mathbf{n}}_{\Gamma}}{\cos\theta_{\rm B}}\,{\rm d}\Gamma. \end{aligned} \quad (33)$$

A more general form of f, useful for distorted lattices, was derived by Apolloni *et al.* (2008). However, for computer-aided calculations, the formal solution (33) is less manageable than equations (15) and (16). Also, in the domain-transformation approach a distortion term with $\mathbf{u} = \mathbf{u}^{\rm rot}$ can be eliminated. Indeed, by introducing two new unknowns $\tilde{D}_{\rm o}$ and $\tilde{D}_{\rm h}$,

$$\tilde{D}_{\rm o,h} = \exp\left[-i\,2K\sin\theta_{\rm B}g(x, \eta)\right]\tilde{d}_{\rm o,h}, \quad (34)$$

where

$$g(x, \eta) = \frac{\alpha}{2}\left\{\frac{x}{\tan\theta_{\rm B}} + \frac{\eta}{T}\left[T + f_2(x) - f_1(x)\right] + f_1(x)\right\}, \quad (35)$$

and by substituting equation (34) into equations (15) and (16) we re-obtain the unperturbed form of the Takagi equations. Now the initial conditions are

$$\tilde{D}_{\rm o}(x,0) = \exp\left[-i\,2K\sin\theta_{\rm B}\,g(x,0)\right] \times \exp\left[-i\frac{K\chi_{\rm o}}{2\cos\theta_{\rm B}}f_1(x)\right]\Phi\left[x,f_1(x)\right], \quad (36)$$

$$\tilde{D}_{\rm h}(x,0) = 0, \quad (37)$$

and the chain of identities (19) becomes

$$D_{\rm o,h}(x,z)|_{\Sigma} = D_{\rm o,h}\left[x,\,T+f_2(x)\right] = \exp\left\{i\frac{K\chi_{\rm o}}{2\cos\theta_{\rm B}}\left[T+f_2(x)\right]\right\} \times \exp\left[i\,2K\sin\theta_{\rm B}\,g(x,\eta=T)\right]\tilde{D}_{\rm o,h}(x,\eta=T). \quad (38)$$

4. Asymmetrically cut crystal

Let us consider the case $f_1(x) = f_2(x) = x\tan\varphi$, shown in Fig. 2, with constraint $|\varphi| < (\pi/2) - |\theta_{\rm B}|$. Then the last term in equation (9) is

$$\frac{\hat{\mathbf{s}}_{\rm o}\cdot\hat{\mathbf{n}}_{\Gamma}}{\cos\theta_{\rm B}}\,{\rm d}\Gamma = (1+\tan\varphi\tan\theta_{\rm B})\,{\rm d}x', \quad (39)$$

where x' is a dummy variable; the product between the Heaviside functions in equations (10) and (11), calculated at $[\Sigma_x(x) - \Gamma_x(x'),\ \Sigma_z(x) - \Gamma_z(x')]$, becomes

$$\begin{aligned}&{\rm H}\left\{\left[\Sigma_z(x)-\Gamma_z(x')\right]|\tan\theta_{\rm B}| + \Sigma_x(x) - \Gamma_x(x')\right\} \times {\rm H}\left\{\left[\Sigma_z(x)-\Gamma_z(x')\right]|\tan\theta_{\rm B}| - \Sigma_x(x) + \Gamma_x(x')\right\} \\ &\quad = {\rm H}\left[T|\tan\theta_{\rm B}| + (x-x')(1+\tan\varphi|\tan\theta_{\rm B}|)\right] \times {\rm H}\left[T|\tan\theta_{\rm B}| - (x-x')(1-\tan\varphi|\tan\theta_{\rm B}|)\right], \end{aligned} \quad (40)$$

and the Dirac delta function in equation (10) becomes

$$\delta\left\{\Sigma_x(x)-\Gamma_x(x') + \left[\Sigma_z(x)-\Gamma_z(x')\right]\tan\theta_{\rm B}\right\} = \delta\left[T\tan\theta_{\rm B}(1+\tan\varphi\tan\theta_{\rm B})^{-1} + x - x'\right]/\left|1+\tan\varphi\tan\theta_{\rm B}\right|. \quad (41)$$

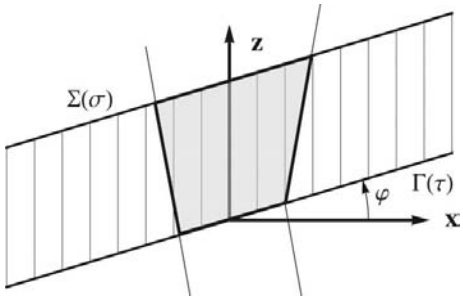

Figure 2
Layout of a parallel-sided asymmetrically cut crystal. The symbol $\Gamma(\tau)$ is the entrance surface, $\Sigma(\sigma)$ is the exit surface and φ, with the constraint $|\varphi| < (\pi/2) - |\theta_{\rm B}|$, is the oriented asymmetry angle. The Borrmann fan is also shown.

The initial condition (8), with $\mathbf{K}_{\rm e} = \mathbf{K}_{\rm o}$, is

$$\Phi(x',z')|_{\Gamma} = A(x', x'\tan\varphi). \quad (42)$$

By substituting equations (39) to (42) into equation (33) and by using the change of variable $x - x' = \zeta$, we have

$$\begin{aligned} D_{\rm o}(x, T+x\tan\varphi;\alpha) &= \exp\left[iKT\frac{\chi_{\rm o}}{2\cos\theta_{\rm B}}(1+\tan\varphi\tan\theta_{\rm B})^{-1}\right] \\ &\times A\left[\frac{T\tan\theta_{\rm B}}{1+\tan\varphi\tan\theta_{\rm B}} + x,\ \left(\frac{T\tan\theta_{\rm B}}{1+\tan\varphi\tan\theta_{\rm B}} + x\right)\tan\varphi\right] \\ &- \frac{K}{4|\sin\theta_{\rm B}|}(\chi_{\rm h}\chi_{-\rm h})^{1/2}\exp\left[iKT\left(\frac{\chi_{\rm o}}{2\cos\theta_{\rm B}} + \alpha\sin\theta_{\rm B}\right)\right] \\ &\times \int_{-T|\tan\theta_{\rm B}|/(1+\tan\varphi|\tan\theta_{\rm B}|)}^{T|\tan\theta_{\rm B}|/(1-\tan\varphi|\tan\theta_{\rm B}|)} \left[\frac{(T+\zeta\tan\varphi)\tan\theta_{\rm B}-\zeta}{(T+\zeta\tan\varphi)\tan\theta_{\rm B}+\zeta}\right]^{1/2} \\ &\times J_1\left\{\frac{K}{2|\sin\theta_{\rm B}|}(\chi_{\rm h}\chi_{-\rm h})^{1/2}\left[(T+\zeta\tan\varphi)^2\tan^2\theta_{\rm B} - \zeta^2\right]^{1/2}\right\} \\ &\times \exp\left\{i\left[\frac{\Re(\chi_{\rm o})\tan\varphi}{2\cos\theta_{\rm B}} + (\cos\theta_{\rm B}+\tan\varphi\sin\theta_{\rm B})\alpha\right]K\zeta\right\} \\ &\times \exp\left[-\frac{\Im(\chi_{\rm o})\tan\varphi}{2\cos\theta_{\rm B}}K\zeta\right]A[x-\zeta,(x-\zeta)\tan\varphi] \\ &\times (1+\tan\varphi\tan\theta_{\rm B})\,{\rm d}\zeta \end{aligned} \quad (43)$$

and

$$\begin{aligned} D_{\rm h}(x, T+x\tan\varphi;\alpha) &= \frac{i}{4}\frac{K\chi_{\rm h}}{|\sin\theta_{\rm B}|}\exp\left[iKT\left(\frac{\chi_{\rm o}}{2\cos\theta_{\rm B}} + \alpha\sin\theta_{\rm B}\right)\right] \\ &\times \int_{-T|\tan\theta_{\rm B}|/(1+\tan\varphi|\tan\theta_{\rm B}|)}^{T|\tan\theta_{\rm B}|/(1-\tan\varphi|\tan\theta_{\rm B}|)} J_0\left\{\frac{K}{2|\sin\theta_{\rm B}|}(\chi_{\rm h}\chi_{-\rm h})^{1/2}\right. \\ &\times \left.\left[(T+\zeta\tan\varphi)^2\tan^2\theta_{\rm B} - \zeta^2\right]^{1/2}\right\} \\ &\times \exp\left\{i\left[\frac{\Re(\chi_{\rm o})\tan\varphi}{2\cos\theta_{\rm B}} + (\cos\theta_{\rm B}+\tan\varphi\sin\theta_{\rm B})\alpha\right]K\zeta\right\} \\ &\times \exp\left[-\frac{\Im(\chi_{\rm o})\tan\varphi}{2\cos\theta_{\rm B}}K\zeta\right]A[x-\zeta,(x-\zeta)\tan\varphi] \\ &\times (1+\tan\varphi\tan\theta_{\rm B})\,{\rm d}\zeta. \end{aligned} \quad (44)$$

From (43) and (44) we note that the most significant effect of the asymmetrical cut is a translation of the rotation angle α by an amount equal to

$$\Delta\theta = -\frac{\Re(\chi_{\rm o})\tan\varphi}{2(1+\tan\varphi\tan\theta_{\rm B})\cos^2\theta_{\rm B}} = \frac{\Re(\chi_{\rm o})(1-\gamma)}{2\sin 2\theta_{\rm B}}, \quad (45)$$

where γ is by definition the asymmetry ratio $\cos(\theta_{\rm B}+\varphi)/\cos(\theta_{\rm B}-\varphi)$. Apart from signs depending on conventions about rotations, the angle $\Delta\theta$ in (45) coincides with the deviation of the reflection-domain centre from the Bragg angle (*cf.* Authier, 2005, p. 85).

5. Numerical simulation

In numerical calculations, carried out by application of *MATHEMATICA* (Wolfram Research, 2009), we have considered the 220 reflections of a silicon lamella, 500 μm thick, and a 17 keV Mo $K\alpha_1$ X-ray source. The angle θ_B has been chosen accordingly and the values of the dielectric susceptibilities, χ_o and $\chi_{\pm h}$, have been taken from Sergey Stepanov's X-ray Server (http://sergey.gmca.aps.anl.gov/). For the z components of the entrance and exit surfaces, $\Gamma_z(x) = f_1(x)$ and $\Sigma_z(x) = T + f_2(x)$, respectively, we chose $f_1(x) = f_2(x) = x\tan\varphi$, and for the distortion term we chose $\mathbf{u} = \mathbf{u}^{\rm rot}$. In this case the function g in (35) reduces to

$$g(x,\eta) = \frac{\alpha}{2}\left[\frac{x}{\tan\theta_B} + \eta + f_1(x)\right], \tag{46}$$

the Takagi–Taupin equations (15, 16) for the field amplitudes (34) reduce to

$$-\sin\theta_B\frac{\partial\tilde{D}_o}{\partial x} + \frac{\cos(\theta_B-\varphi)}{\cos\varphi}\frac{\partial\tilde{D}_o}{\partial\eta} = \frac{i}{2}K\chi_{-h}\tilde{D}_h \tag{47}$$

$$\sin\theta_B\frac{\partial\tilde{D}_h}{\partial x} + \frac{\cos(\theta_B+\varphi)}{\cos\varphi}\frac{\partial\tilde{D}_h}{\partial\eta} = \frac{i}{2}K\chi_h\tilde{D}_o, \tag{48}$$

and the initial conditions (36, 37) become

$$\tilde{D}_o(x,0) = \exp\left[-iK\alpha x(1+\tan\varphi\tan\theta_B)\cos\theta_B\right] \times \exp\left(-i\frac{K\chi_o}{2\cos\theta_B}x\tan\varphi\right)\Phi(x, x\tan\varphi), \tag{49}$$

$$\tilde{D}_h(x,0) = 0. \tag{50}$$

The X-ray source has been modelled as a monochromatic wave $A(x,z)\exp(i\,\mathbf{K}_e\cdot\mathbf{r})$ having width w = 1 mm, where (see Fig. 3)

$$A(x,z) = p(x + z\tan\theta_B) \tag{51}$$

and

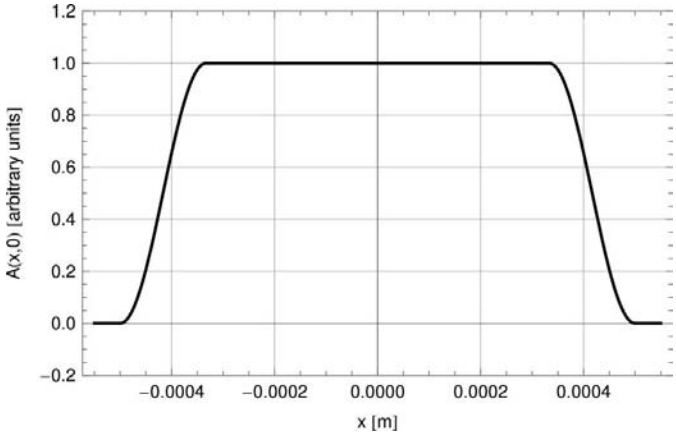

Figure 3
Plane wave factor $A(x,0) = p(x)$ used in numerical calculations.

$$p(x) = \begin{cases} \cos^2(3\pi x/w) & \text{if } -w/2 \le x < -w/3, \\ 1 & \text{if } -w/3 \le x \le w/3, \\ \cos^2(3\pi x/w) & \text{if } -w/3 < x \le w/2, \\ 0 & \text{otherwise.} \end{cases} \tag{52}$$

5.1. Rocking curves

In order to validate relation (45) between the peak shift $\Delta\theta$ and the asymmetry angle φ, we considered different cases, the asymmetry angle φ ranging from $-7\theta_B$ to $7\theta_B$, and the rotation angle α from −25 μrad to 25 μrad. As an example of output, in Figs. 4, 5 and 6 we show the single-crystal rocking curves $I_h(\alpha;\varphi) = \int_\Sigma |D_h(\Sigma_x, \Sigma_z; \alpha, \varphi)|^2\,\hat{\mathbf{s}}_h\cdot\hat{\mathbf{n}}_\Sigma\,d\Sigma$ for φ = 0 rad, $\varphi = 2\theta_B$ and $\varphi = -5\theta_B$, respectively. When φ = 0 rad (Fig. 4), the simulated rocking curve is rigorously symmetric, as can easily be deduced from equations (44) and from the symmetry properties of $A(x,0)$, equation (51), brought about by $p(x)$, equation (52); in other cases, with a greater modulus of the asymmetry angle $|\varphi|$, the asymmetry of the rocking curve is greater. The shift of the central peaks, or of valleys, of all the simulated rocking curves is shown in Fig. 7 and agrees with the value obtained for $\Delta\theta$ by equation (45). If we substitute the first-order expansion in φ of (45),

$$\Delta\theta \simeq -\frac{\Re(\chi_o)}{2\cos^2\theta_B}\varphi, \tag{53}$$

into the differential form of the Bragg law

$$\Delta\lambda/\lambda = \Delta\theta/\tan\theta_B, \tag{54}$$

we have the formula

$$\frac{\Delta\lambda}{\lambda} \simeq -\frac{\Re(\chi_o)}{\sin 2\theta_B}\varphi \tag{55}$$

to estimate measurement errors in wavelength λ or to impose an upper limit on φ. However, it is necessary to make further numerical investigations with higher-energy incoming beams and thicker crystals.

5.2. Fringe-phase effects

In order to understand the effects of an asymmetrical cut on the measurement of the lattice parameter by an LLL X-ray interferometer, we have considered a simplified system consisting of a single, asymmetrically cut, perfect lamella and two identical incoming beams, the parameters of which have been chosen according to equations (51) and (52). This composite problem can be solved by studying separately the two single-beam propagations, one in which a beam comes from the right-hand side ($\theta_B > 0$) and the other in which a beam comes from the left-hand side ($\theta_B < 0$), and then by recombining the two solutions. Let us introduce the self-explaining notations $\tilde{d}_o^{\theta_B>0}$, $\tilde{d}_o^{\theta_B<0}$, and similarly for h waves, and consider first the case $\theta_B > 0$. In this case the Takagi–Taupin equations (15) and (16), with $\mathbf{u} = 0$, reduce to equations (47) and (48) for the unknown $\tilde{d}_o^{\theta_B>0}$ and $\tilde{d}_h^{\theta_B>0}$, with the initial conditions

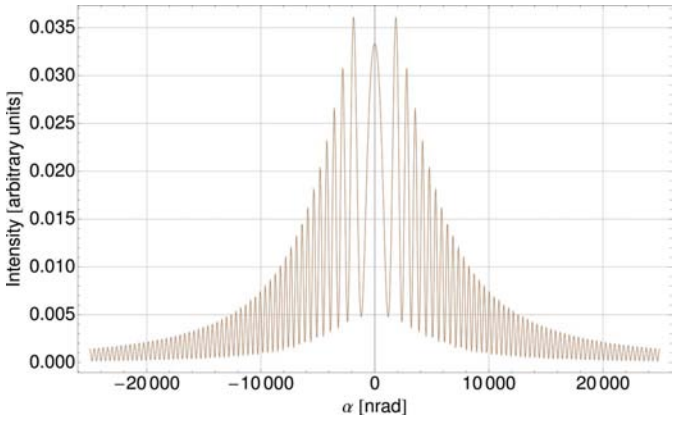

Figure 4
Calculated rocking curves of 220 reflections for a symmetrically cut 500 µm-thick silicon crystal. A beam of 17 keV X-rays from a conventional Mo source illuminates the entrance surface.

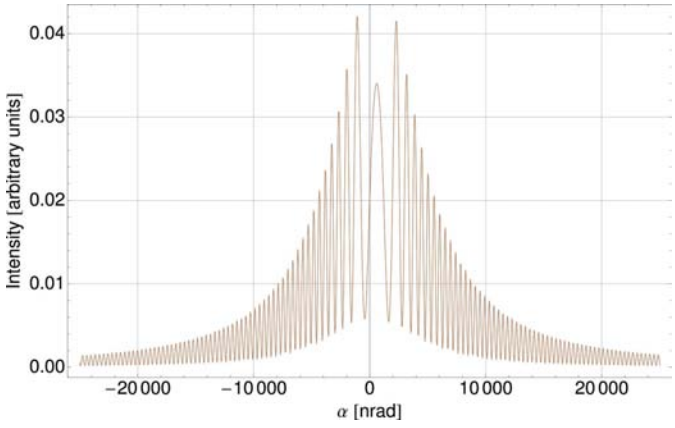

Figure 5
Calculated rocking curves of 220 reflections for an asymmetrically cut silicon crystal. The crystal thickness is 500 µm. The asymmetry angle is $2\theta_B$. A beam of 17 keV X-rays from a conventional Mo source illuminates the entrance surface.

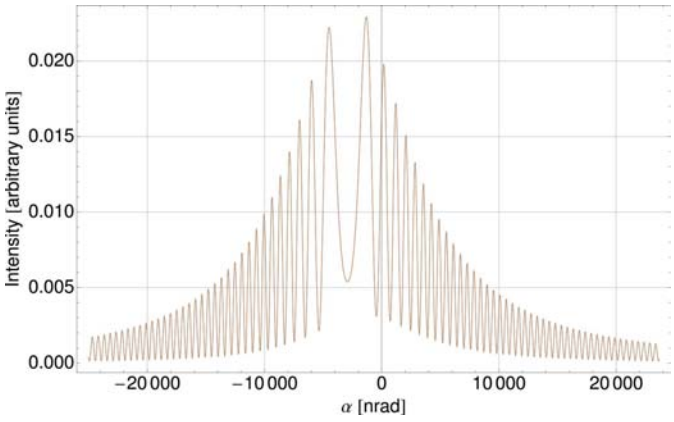

Figure 6
Calculated rocking curves of 220 reflections for an asymmetrically cut silicon crystal. The crystal thickness is 500 µm. The asymmetry angle is $-5\theta_B$. A beam of 17 keV X-rays from a conventional Mo source illuminates the entrance surface.

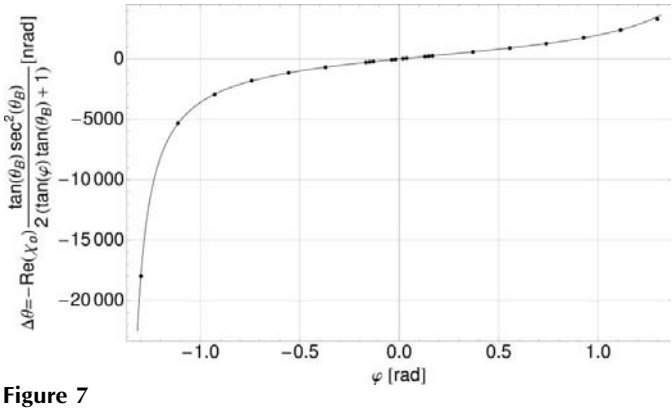

Figure 7
Deviation of the reflection-domain centre $\Delta\theta$ *versus* asymmetry angle φ. Circles refer to the peak shift of simulated rocking curves of 220 reflections for asymmetrically cut silicon crystals. A beam of 17 keV X-rays from a conventional Mo source illuminates the entrance surface.

$$\tilde{d}_{\rm o}^{\theta_{\rm B}>0}(x,0)=\exp\left(-i\frac{K\chi_{\rm o}}{2\cos\theta_{\rm B}}x\tan\varphi\right)p(x+x\tan\varphi\tan\theta_{\rm B}), \tag{56}$$

$$\tilde{d}_{\rm h}^{\theta_{\rm B}>0}(x,0)=0. \tag{57}$$

Now, let us consider the case $\theta_{\rm B}<0$. We must observe that, when we make the transformation $\theta_{\rm B}\rightarrow-\theta_{\rm B}$ in equations (47) and (48) and in initial conditions (56, 57), the solutions $(\tilde{d}_{\rm o}^{\theta_{\rm B}<0}, \tilde{d}_{\rm h}^{\theta_{\rm B}<0})$ of the new system also satisfy the old system (47, 48) for $(\tilde{d}_{\rm o}^{\theta_{\rm B}>0}, \tilde{d}_{\rm h}^{\theta_{\rm B}>0})$ with the initial conditions

$$\tilde{d}_{\rm o}^{\theta_{\rm B}>0}(x,0)=0, \tag{58}$$

$$\tilde{d}_{\rm h}^{\theta_{\rm B}>0}(x,0)=\exp\left(-i\frac{K\chi_{\rm o}}{2\cos\theta_{\rm B}}x\tan\varphi\right)p(x-x\tan\varphi\tan\theta_{\rm B}), \tag{59}$$

provided that we make the change o $\leftrightarrow$ h, that is the assignment $(\tilde{d}_{\rm o}^{\theta_{\rm B}>0}, \tilde{d}_{\rm h}^{\theta_{\rm B}>0}) = (\tilde{d}_{\rm h}^{\theta_{\rm B}<0}, \tilde{d}_{\rm o}^{\theta_{\rm B}<0})$. By exploiting this observation and restoring the previous meaning of the symbols, we can conclude that the linear superposition $(\tilde{d}_{\rm o}^{\theta_{\rm B}>0}+\tilde{d}_{\rm h}^{\theta_{\rm B}<0}, \tilde{d}_{\rm h}^{\theta_{\rm B}>0}+\tilde{d}_{\rm o}^{\theta_{\rm B}<0})$ of the solutions of the two above cases satisfy equations (47) and (48) with the boundary conditions (56, 59). However, the conventionally transmitted o wave, *i.e.* the first component of the above pair, and the conventionally reflected h wave, *i.e.* the second component, are not the same because the left–right simmetry is broken by the asymmetrical cut angle $\varphi\neq0$; the symmetry laws are

$$\tilde{d}_{\rm o}^{\theta_{\rm B}>0}(x,\eta;\varphi)=\tilde{d}_{\rm o}^{\theta_{\rm B}<0}(-x,\eta;-\varphi), \tag{60}$$

$$\tilde{d}_{\rm h}^{\theta_{\rm B}<0}(x,\eta;\varphi)=\tilde{d}_{\rm h}^{\theta_{\rm B}>0}(-x,\eta;-\varphi), \tag{61}$$

and, obviously, for the sum we have

$$\begin{aligned}&\tilde{d}_{\rm o}^{\theta_{\rm B}>0}(x,\eta;\varphi)+\tilde{d}_{\rm h}^{\theta_{\rm B}<0}(x,\eta;\varphi)\\&\quad=\tilde{d}_{\rm h}^{\theta_{\rm B}>0}(-x,\eta;-\varphi)+\tilde{d}_{\rm o}^{\theta_{\rm B}<0}(-x,\eta;-\varphi).\end{aligned} \tag{62}$$

Let us confine ourselves to the conventionally transmitted o wave. Apart from multiplicative constants, the flux of the Poynting vector $I_{\rm o}$, in terms of the previous fields $D_{\rm o}$ and $D_{\rm h}$, is

$$I_{\rm o}(\varphi) = \int_{\Sigma} |D_{\rm o}^{\theta_{\rm B}>0}(\Sigma_x, \Sigma_z; \varphi) + D_{\rm h}^{\theta_{\rm B}<0}(\Sigma_x, \Sigma_z; \varphi)|^2 \, \hat{\mathbf{s}}_{\rm o} \cdot \hat{\mathbf{n}}_{\Sigma} \, {\rm d}\Sigma, \quad (63)$$

which, by exploitation of (19), can be written in terms of the new fields $\tilde{d}_{\rm o}$ and $\tilde{d}_{\rm h}$ as

$$I_{\rm o}(\varphi) = \int_{\Sigma} \exp\left\{-\frac{K\Im(\chi_{\rm o})}{\cos\theta_{\rm B}}\left[T + f_2(x)\right]\right\} \times |\tilde{d}_{\rm o}^{\theta_{\rm B}>0}(x, T; \varphi) + \tilde{d}_{\rm h}^{\theta_{\rm B}<0}(x, T; \varphi)|^2 \, \hat{\mathbf{s}}_{\rm o} \cdot \hat{\mathbf{n}}_{\Sigma} \, {\rm d}\Sigma. \quad (64)$$

By introduction of the following definitions,
(i) offset

$$\begin{aligned}\mathcal{I}_{\rm o}(\varphi) &= \int_{\Sigma} \left[|D_{\rm o}^{\theta_{\rm B}>0}(\Sigma_x, \Sigma_z; \varphi)|^2 + |D_{\rm h}^{\theta_{\rm B}>0}(\Sigma_x, \Sigma_z; \varphi)|^2\right] \hat{\mathbf{s}}_{\rm o} \cdot \hat{\mathbf{n}}_{\Sigma} \, {\rm d}\Sigma \\ &= \int_{\Sigma} \exp\left\{-\frac{K\Im(\chi_{\rm o})}{\cos\theta_{\rm B}}\left[T + f_2(x)\right]\right\} \times \left[|\tilde{d}_{\rm o}^{\theta_{\rm B}>0}(x, T; \varphi)|^2 + |\tilde{d}_{\rm h}^{\theta_{\rm B}>0}(x, T; \varphi)|^2\right] \hat{\mathbf{s}}_{\rm o} \cdot \hat{\mathbf{n}}_{\Sigma} \, {\rm d}\Sigma, \end{aligned} \quad (65)$$

(ii) modulation

$$\begin{aligned}\Xi_{\rm o}(\varphi) &= \int_{\Sigma} \overline{D_{\rm o}^{\theta_{\rm B}>0}(\Sigma_x, \Sigma_z; \varphi)} \times D_{\rm h}^{\theta_{\rm B}<0}(\Sigma_x, \Sigma_z; \varphi) \, \hat{\mathbf{s}}_{\rm o} \cdot \hat{\mathbf{n}}_{\Sigma} \, {\rm d}\Sigma \\ &= \int_{\Sigma} \exp\left\{-\frac{K\Im(\chi_{\rm o})}{\cos\theta_{\rm B}}\left[T + f_2(x)\right]\right\} \times \overline{\tilde{d}_{\rm o}^{\theta_{\rm B}>0}(x, T; \varphi)} \, \tilde{d}_{\rm h}^{\theta_{\rm B}<0}(x, T; \varphi) \, \hat{\mathbf{s}}_{\rm o} \cdot \hat{\mathbf{n}}_{\Sigma} \, {\rm d}\Sigma, \end{aligned} \quad (66)$$

(iii) extra phase

$$\Phi_{\rm o}(\varphi) = \arg\left[\Xi_{\rm o}(\varphi)\right], \quad (67)$$

and (iv) visibility

$$\Gamma_{\rm o}(\varphi) = 2\,|\Xi_{\rm o}(\varphi)|/\mathcal{I}_{\rm o}(\varphi), \quad (68)$$

the flux $I_{\rm o}$ can be decomposed in the more significant form

$$I_{\rm o}(\varphi) = \mathcal{I}_{\rm o}(\varphi)\left\{1 + \Gamma_{\rm o}(\varphi)\cos\left[\Phi_{\rm o}(\varphi)\right]\right\}. \quad (69)$$

If we operate analogously with the conventionally transmitted h wave, we obtain a similar expression for $I_{\rm h}$. As we are considering only one lamella, the two fluxes are connected by a simple inversion operation, *i.e.* $I_{\rm h}(\varphi) = I_{\rm o}(-\varphi)$; however, the same does not hold true for polylithic interferometers. The calculated flux of the Poynting vector $I_{\rm o}(\varphi)$ and the two components $\mathcal{I}_{\rm o}(\varphi)$ and $2|\Xi_{\rm o}(\varphi)|\cos[\Phi_{\rm o}(\varphi)]$ are shown in Fig. 8; for the phase $\Phi_{\rm o}(\varphi)$ and the visibility $\Gamma_{\rm o}(\varphi)$, see Fig. 9. A magnification of $\Phi_{\rm o}(\varphi)$ is also shown in Fig. 10.

If we take into account a translation s of the lamella with its phase term $(2\pi/d_{220})s$, and assume that the total fringe phase can be decomposed into a linear superposition of two terms, and the other terms can be replaced by constants, *i.e.* C_0 for $\mathcal{I}_{\rm o}(\varphi)$ and C_1 for $\Gamma_{\rm o}(\varphi)$, then the flux of the Poynting vector can be approximated as

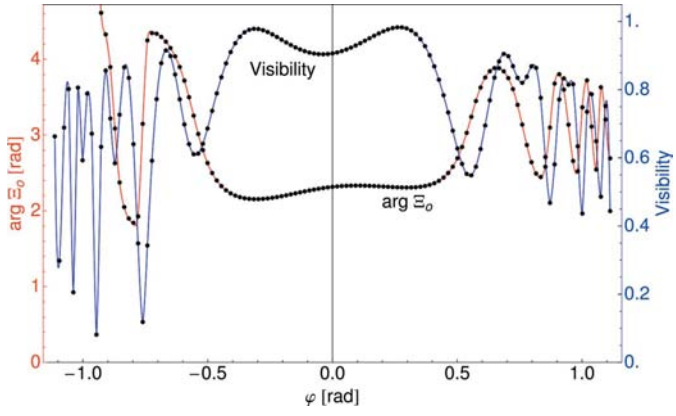

Figure 9
Numerical solution of Takagi–Taupin equations. Visibility $\Gamma_{\rm o}(\varphi) = 2|\Xi_{\rm o}(\varphi)|/\mathcal{I}_{\rm o}(\varphi)$ and extra-phase term $\Phi_{\rm o} = \arg(\Xi_{\rm o})$ of signal *versus* asymmetry angle φ. A 500 µm-thick single silicon lamella is illuminated by two beams of 17 keV X-rays from a conventional Mo source.

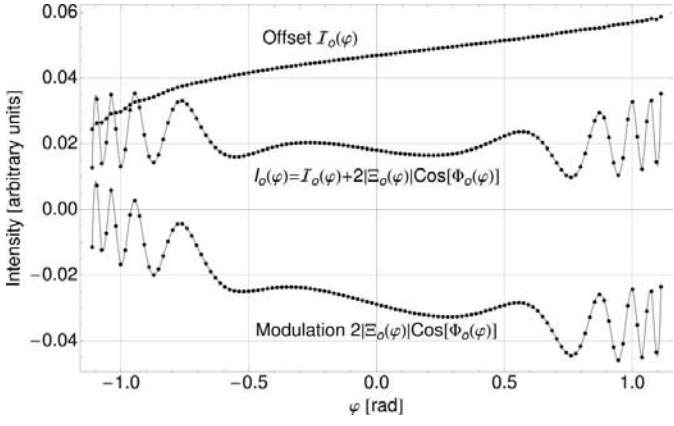

Figure 8
Numerical solution of Takagi–Taupin equations. Flux of Poynting vector, offset and modulation, *versus* asymmetry angle φ. A 500 µm-thick single silicon lamella is illuminated by two beams of 17 keV X-rays from a conventional Mo source.

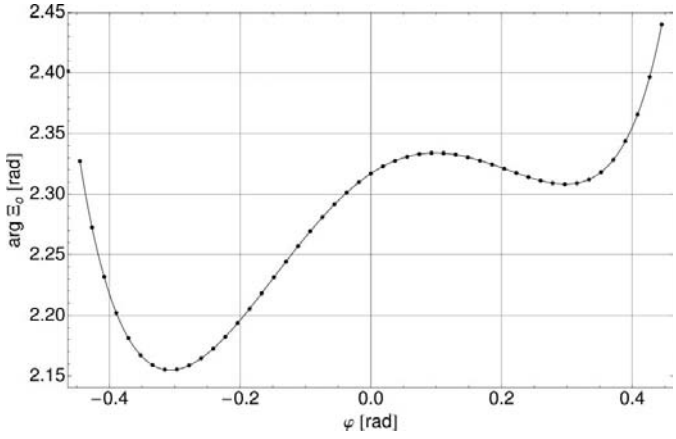

Figure 10
Numerical solution of Takagi–Taupin equations. Magnification of the extra-phase term $\Phi_{\rm o} = \arg(\Xi_{\rm o})$ of signal *versus* asymmetry angle φ.

$$I_o(\varphi) \simeq C_0 + C_1 \cos\left\{\frac{2\pi}{d_{220}} s + \Phi_o[\varphi(s)]\right\}. \quad (70)$$

The fringe-phase excess, at the end of a lamella displacement Δs, brings about a relative variation of the measured period

$$\frac{\Delta d_{220}}{d_{220}} \simeq \frac{\Delta \Phi_o}{2\pi} \frac{d_{220}}{\Delta s}, \quad (71)$$

where $\Delta\Phi_o \simeq (d\Phi_o/d\varphi)\Delta\varphi$. If we suppose a surface roughness with $\Gamma_z(x) \simeq \Sigma_z(x) \simeq A \sin[(2\pi/L)x]$, where $A = 5$ µm and $L = 100$ µm (Massa *et al.*, 2009), the variation $\Delta\varphi$ of the asymmetry angle $\varphi = \arctan(d\Gamma_z/dx)$ will be approximately 0.2π rad and $d\Phi_o/d\varphi \simeq 0.4$. By imposing $\Delta d_{220}/d_{220} \simeq 10^{-9}$ and substituting the just mentioned values into (71), the displacement Δs must be of the order of 1 cm.

6. Conclusions

We studied X-ray and γ-ray propagation in crystals having arbitrary surfaces. Exact solutions of the relevant Takagi–Taupin equations have been given in the form of integrals by use of the Riemann–Green method. In the asymmetrical-cut case, the exact solutions have been exploited to re-obtain a known relation between the reflection-domain centre and the asymmetry angle. Successively, in order to solve the Takagi–Taupin equations numerically, we introduced a change of variable which transforms an irregular domain into a rectangle. After a comparison between two different approaches to small crystal rotation, we studied numerically the rocking curves for parallel-sided, asymmetrically cut, single crystals. The peak shifts of the simulated rocking curves were in agreement with the expected values, which had been calculated previously by use of the just mentioned relation. A link between the relative uncertainty in incoming-beam wavelength and asymmetry angle has also been given.

The effect of surface roughness on the phase of an interferometer signal has been outlined by a study of the extra-phase term brought about by a constant asymmetry angle. We have estimated an analyser displacement of about 1 cm so that a surface roughness described by $\sim A \sin[(2\pi/L)x]$, where $A = 5$ µm and $L = 100$ µm, does not cause a deviation larger than the targeted relative error 10^{-9}. The study of more realistic cases, with thicker crystals, higher energy and polylithic systems, will be the subject of future investigations.

This work was supported by the Museo Storico della Fisica e Centro Studi e Ricerche 'Enrico Fermi', Rome, by the Regione Piemonte and by the Compagnia San Paolo, Turin. We wish to thank Gianfranco Zosi for useful suggestions and Giovanni Mana for helpful discussions.

References

Apolloni, A., Mana, G., Palmisano, C. & Zosi, G. (2008). *Acta Cryst.* A**64**, 549–559.
Authier, A. (2005). *Dynamical Theory of X-ray Diffraction*, 3rd ed. Oxford: IUCr/Oxford University Press.
Authier, A. & Simon, D. (1968). *Acta Cryst.* A**24**, 517–526.
Becker, P. (2003). *Metrologia*, **40**, 366–375.
Becker, P., De Bièvre, P., Fujii, K., Glaeser, M., Inglis, B., Luebbig, H. & Mana, G. (2007). *Metrologia*, **44**, 1–14.
Becker, P., Jentschel, M., Mana, G. & Zosi, G. (2007). In *Metrology & Fundamental Constants, Proceedings of the International School of Physics 'E. Fermi'*, course CLXVI, edited by T. W. Haench, S. Leschiutta & A. J. Wallard. Amsterdam: IOS Press.
Flowers, J. (2004). *Science*, **64**, 1324–1330.
Gronkowski, J. (1991). *Phys. Rep.* **206**, 1–41.
Mana, G. & Montanari, F. (2004). *Acta Cryst.* A**60**, 40–50.
Massa, E., Mana, G. & Jentschel, M. (2005). Experimental Report 3-03-673. Institut Laue-Langevin, Grenoble, France.
Massa, E., Mana, G., Kuetgens, U. & Ferroglio, L. (2009). *New J. Phys.* **11**, 053013.
Materna, T., Bruyneel, B., Jolie, J., Linnemann, A., Warr, N., Börner, H. G., Jentschel, M., Mutti, P. & Simpson, G. (2006). *Nucl. Instrum. Methods Phys. Res. A*, **569**, 890–893.
Mills, I. M., Mohr, P. J., Quinn, T. J., Taylor, B. N. & Williams, E. R. (2005). *Metrologia*, **42**, 71–81.
Palmisano, C. & Zosi, G. (2005). *Am. J. Phys.* **73**, 860–870.
Robinson, J. (2006). *Sci. Am.* (December), pp. 102–109.
Sommerfeld, A. (1964). *Partial Differential Equations in Physics.* New York: Academic Press.
Takagi, S. (1962). *Acta Cryst.* **15**, 1311–1312.
Takagi, S. (1969). *J. Phys. Soc. Jpn*, **26**, 1239–1253.
Taupin, D. (1964). *Bull. Soc. Fr. Minér. Crist.* **60**, 469–511.
Thorkildsen, G. & Larsen, H. B. (1998). *Acta Cryst.* A**54**, 172–185.
Wolfram Research (2009). *Mathematica.* Version 7.0. Wolfram Research, Inc., 100 Trade Center Drive, Champaign, IL 61820–7237, USA.